

# Classic and Robust PID Heading Control of an Unmanned Robotic Airship\*

J. Carvalho, E. de Paiva, J. Azinheira, P. Ferreira, J. Ramos, S. Bueno, M. Bergerman, S. Maeta, L. Mirisola, B. Faria, A. Elfes

Robotics and Computer Vision Laboratory-LRV/ITI  
Rod. Dom Pedro I, Km 143,6, 13089-500, Campinas-SP, Brazil  
e-mail: samuel.bueno@iti.br

**Abstract.** Project AURORA aims at the development of an unmanned airship capable of autonomous flight over user-defined locations for aerial inspection and imagery acquisition. The guidance control strategy is based on a path tracking error generation methodology that takes into account both the distance and the angular errors of the airship with respect to the desired trajectory. The control strategy uses a PI controller for the tail surfaces' deflection. This article focuses on the heading controller, which is an internal component of the guidance controller for trajectory path following. The gains of the heading controller are designed using an  $\mathcal{H}_2/\mathcal{H}_\infty$  guaranteed cost PD design technique. The performance of the optimized PD controller is then compared with a non-optimized proportional (P) controller, which was used in a experimental flight.

## 1 Introduction

A great interest in the utilization of unmanned aerial vehicles appeared in the last decade, due to their potential application in varied tasks such as surveillance, advertising, monitoring, inspection, exploration, and research roles. A new and special attention has been given to the use of unmanned aerial vehicles in environmental applications, such as bio-diversity, ecological, climatological, and agricultural research and monitoring, among others [2].

In this context the authors are currently developing Project AURORA (Autonomous Unmaned Remote Monitoring Robotic Airship) which focuses on the development of the sensing, control, navigation, and inference technologies required for semi-autonomous operation of unmanned robotic airships for aerial inspection [2], [16], [17], [18], [1]. AURORA is conceived as a multi-phase project, the current one being AURORA I, which aims at establishing the underlying technologies and at performing low demanding applications.

The lighter-than-air platform of AURORA I is the AS800 by Airspeed Airships, a non-rigid, 9 m long, 2.25 m in diameter, 24  $m^3$  airship (Figure 1). The airship control actuators are its deflection surfaces and two-stroke internal combustion engines. The four deflection surfaces at the stern, arranged in an 'X' shape, generate the equivalent rudder and elevator commands of the classical + tail, with allowable deflections situated in the range -25 to +25 deg. The two engines on the sides of the gondola can be vectorized from 0 to +90 degrees up.

This article focuses on the development of a heading controller for AURORA's airship at medium to high airspeed, using the  $\mathcal{H}_2/\mathcal{H}_\infty$  guaranteed cost PD design technique proposed in [7]. The heading controller is used as an internal component of the guidance controller for trajectory path following [5]. Another  $\mathcal{H}_\infty$  approach for the heading control problem, is presented in [10], but without considering multi-objective optimization for multiple linearized plants.

The objectives of the heading control system are the tracking of a reference input and disturbance rejection, in terms of attenuation of the perturbation and the reduction of the amount of rolling oscillation during yaw maneuvering and turbulence caused by the slightly damped poles of the lateral dynamics.

The resulting optimized gains is then compared with the non-optimized ones used in a successful airship autonomous flight achieved through a set of pre-defined points, one of the first of its kind in the literature.

\* Dr. P. Ferreira is with the Department of Telematics, UNICAMP, Brazil; Dr. J. Azinheira is with the Department of Mechanical Engineering, IST, Lisbon, Portugal, and Dr. A. Elfes is with the FAW Laboratory at Ulm, Germany. The remaining authors are with the Robotics and Computer Vision Laboratory.



Fig. 1. AURORA I airship AS800.

This flight was achieved with the same PI control-based guidance strategy for the trajectory path following used in the optimization problem formulation. The horizontal trajectory is controlled automatically by the on-board system, while altitude is controlled manually by the ground pilot, but through smooth actions.

## 2 Airship Dynamic Model and Linearized System

In this section we briefly review the nonlinear dynamic model representing the airship. A more detailed presentation can be found in [3] and [9].

The dynamic model describes the motion in a system of orthogonal body axes fixed in the airship, with the origin at the Center of Volume (CV), assumed to coincide with the gross Center of Buoyancy (CB). The attitude of this body fixed frame with respect to an Earth-fixed frame is obtained through a transformation matrix that may be expressed through the Euler roll, pitch and yaw angles  $(\phi, \theta, \psi)$ .

The linear  $(U, V, W)$  and angular  $(P, Q, R)$  velocities of the vehicle with respect to the Earth frame is given in the Body frame, and constitute the vector of inertial velocities  $\mathbf{x} = [U, V, W, P, Q, R]$ .

The dynamic model can be stated as:

$$\overline{\mathbf{M}}_a \dot{\mathbf{x}} = \overline{\mathbf{F}}_a + \overline{\mathbf{F}}_g + \overline{\mathbf{F}}_p + \overline{\mathbf{F}}_k \quad (1)$$

with the generalized forces produced by aerodynamics  $(\overline{\mathbf{F}}_a)$ , gravity  $(\overline{\mathbf{F}}_g)$ , propulsion  $(\overline{\mathbf{F}}_p)$ , and kinematic inertia  $(\overline{\mathbf{F}}_k)$ , and the generalized apparent mass matrix  $\overline{\mathbf{M}}_a$  that includes both the airship actual inertia as well as the virtual inertia elements associated with the dynamics of buoyant vehicles [3].

Based on this 6 DOF non-linear model, a Simulink-based simulation and control development environment was built, in order to allow the design and validation of control and navigation strategies [6]. As actuators, the AS800 is equipped with deflection surfaces and thrusters. The 'X'-shaped deflection surfaces of the tail generate the equivalent rudder and elevator commands of the classical '+' tail, with allowable deflections from  $-25^\circ$  to  $+25^\circ$ . The engines can be vectored from  $0$  to  $+90^\circ$  up (Figure 2). The rudder and elevator are responsible for direction control (left and right, up and down) and their behavior is due to aerodynamic forces produced at medium to high speeds. The thrusters generate the necessary thrust for the airship motion. Its vectoring is used for vertical load compensation and to provide vertical forces in low speeds. The airship has also an electrical stern thruster used mainly during hover.

The complexity of the non-linear dynamic equations justify the search for a linear simplified version that is very important for the control systems design. The linearization of the motion equations are made for trimmed conditions around equilibrium, which is frequently that of horizontal straight flight. In such conditions, the equations are written for the perturbation vector  $x$  of the states around the equilibrium value  $X$ , and the perturbed inputs  $u$  and  $w$ . The linearized models depend on the point chosen for the linearization, and in particular of the total airspeed  $V_{total0}$  and altitude  $h_0$  chosen.

It is a general assumption to consider two independent (decoupled) movements: the movement in the vertical plane, named longitudinal, and that in the horizontal plane, named lateral.

In the lateral case, the state vector considered to represent the model is  $x = [v, p, r, \phi]$  and the input vector is given by  $u = \zeta$ , the angular deflection of the rudder surface, where the lower case letters represent the perturbations around the nominal values. For the heading problem, the output considered is the yaw rate. Therefore, the lateral dynamic approach is given by:

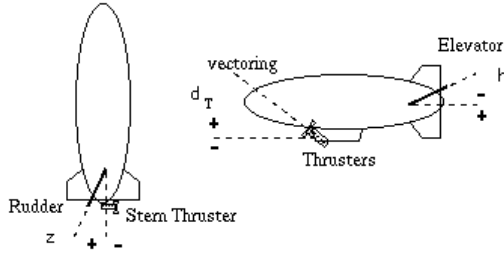


Fig. 2. Airship actuators.

$$\begin{cases} \dot{x} = Ax + Bu + Ew \\ y = Cx \end{cases} \quad (2)$$

The vector  $w$  of the perturbation is a stochastic turbulence, generated by a Dryden model, with three white noise inputs [8].

## 2.1 Path Tracking Problem

One important navigation problem is the flight path following of the vehicle through a set of pre-defined points in latitude/longitude.

The problem of path tracking for autonomous vehicles appears as a good application for very different control strategies [11], [18], [15], [1]. Path tracking is a typical regulation problem, where one looks for a command input able to reduce the path tracking error for a given mission path.

For the airship, allowable mission paths are defined as a sequence of straight lines and circle arcs between the given way-points. The heading change at each way-point (between consecutive segments) may vary in the  $\pm 180^\circ$  range and the distance between the actual airship position and the mission path is to be minimized in all cases.

In the path tracking control strategy presented in [5], it is considered that the longitudinal motion is maintained at a constant altitude and airspeed and acceptably decoupled from the lateral motion, which is a common assumption in aerial vehicle control. The variables used in such a strategy are depicted in Figure 3, where  $\delta$  is the distance error to the desired path,  $\epsilon$  is the angular error,  $V$  is the ground speed, and  $\Psi_{traj}$  is the heading angle of the trajectory with respect to the north-east reference frame.

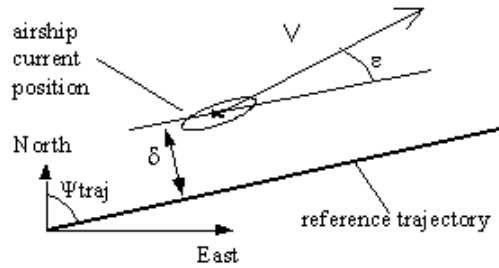


Fig. 3. Path tracking signals.

Considering a flight with small pitch and roll angles, for constant speed and small angular error  $\epsilon$ , the following simplified path tracking linearized model results:

$$\begin{aligned} d\delta/dt &= V \sin(\epsilon) \approx V_o \epsilon \\ d\epsilon/dt &= R \end{aligned} \quad (3)$$

where  $V_o$  is the reference ground speed considered for design purposes and  $R$  is the yaw rate.

In order to accommodate both the distance and angular errors in a single equation, a look-ahead error,  $\delta_a$ , may be estimated some time ahead of the actual position:

$$\delta_a \approx \delta + V_o \Delta_t \epsilon \quad (4)$$

where  $\Delta_t$  is the prediction horizon. This strategy has already been successfully used for the guidance of both unmanned aircraft [15] and ground mobile robots [13].

### 3 Guidance Control Strategy

This guidance methodology is part of AURORA's overall airship control architecture, described in [6]. The control structure consists of a heading control inner loop and a path-tracking outer loop [5]. It is shown in Figure 4, where  $\Psi$  is the airship heading (*yaw*) angle. The control signal is the rudder deflection ( $\zeta$ ).

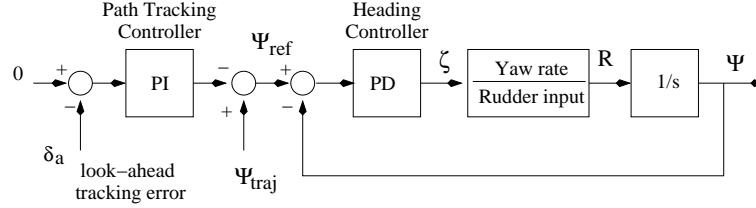


Fig. 4. PI control block diagram.

The reference signal  $\Psi_{ref}$  is composed by the trajectory heading angle  $\Psi_{traj}$  and the output of the path-tracking controller, consisting of a PI controller with an anti-wind up strategy to avoid saturation of the integral term.

The  $\Psi_{ref}$  is sent as reference to the controller of the rudder surface, which was initially set as a proportional controller. However, experiments has shown that only a proportional gain, despite giving a reasonable tracking error, do not assure a good performance in terms of the overall airship behavior. For instance, the airship tend to have a large excursion of the roll angle during the changing of direction, which would make the realization of inspection missions a difficult task, specially those depending on acquisition of videos. Thus, we search for a control structure which preserves the simplicity of PID controller while providing a good performance of the tracking error, and decreasing the rolling during the changing of direction of  $\Psi_{ref}$ . An approach to doing so is to find a controller that minimizes the norm of the closed-loop transfer function from the reference and gust inputs to the system outputs (control signal and tracking error). This is the subject of Section 4, where a PD structure is adopted.

For control system synthesis purpose, in the sequel the linearized transfer functions from rudder to yaw rate are used,  $P_6$ ,  $P_8$  and  $P_{10}$  respectively for 6, 8 and 10 m/s airspeeds.

$$P_6 = \frac{-1.076s^3 - 1.569s^2 - 5.498s - 3.769}{s^4 + 4.887s^3 + 9.028s^2 + 20.59s + 7.015}$$

$$P_8 = \frac{-1.881s^3 - 3.682s^2 - 10.34s - 8.817}{s^4 + 6.533s^3 + 12.64s^2 + 28.44s + 12.49}$$

$$P_{10} = \frac{-2.905s^3 - 7.127s^2 - 17.45s - 17.06}{s^4 + 8.186s^3 + 17.29s^2 + 37.25s + 19.6}$$

## 4 $\mathcal{H}_2/\mathcal{H}_\infty$ Problem Formulation

In this section, we describe the matrix representation of the closed-loop system, that considers the PD gains for the optimization problem of the heading control inner loop, according to the methodology presented in [7].

Consider the linear system of equation (2) with  $A \in \mathbb{R}^{4 \times 4}$ ,  $B \in \mathbb{R}^{4 \times 1}$ ,  $E \in \mathbb{R}^{4 \times 4}$ , and  $C \in \mathbb{R}^{1 \times 4}$ . We have considered the set of three linearized models  $P_6$ ,  $P_8$  and  $P_{10}$ , such that the triple  $A, B, C$  belongs to the following set:

$$\mathcal{P} = \{\langle A_i, B_i, C_i \rangle, i = 1, \dots, 3\}$$

The goal of the controller design is to control the output  $y(t)$  in such a way that the error w.r.t. a reference input  $y_{ref}(t)$  and the disturbance  $w(t)$  in the output are simultaneously minimized. The control action for the PD compensator is characterized by the equations:

$$e = y_{ref} - y, \quad u = K_p e + K_d \frac{de}{dt}$$

Due to the non causal characteristic of the derivative term, this problem is more conveniently formulated in terms of an augmented states equation. Define two state variables:

$$f = \int e dt, \quad \dot{y}_{ref_c} = -a y_{ref_c} + a y_{ref}$$

in which  $a \gg \max(|\lambda(A)|)$  for all  $A \in \mathcal{P}$ . The auxiliary variable  $y_{ref_c}(t)$  is introduced to make causal the compensator derivative term. Then, the output error must be redefined as:

$$e = y_{ref_c} - y$$

Now define the matrices:

$$\bar{A} = \begin{bmatrix} A & 0 \\ 0 & -a \end{bmatrix} \quad \bar{B} = \begin{bmatrix} B \\ 0 \end{bmatrix} \quad \bar{G} = \begin{bmatrix} -C & 1 \\ -CA & -a \end{bmatrix} \quad \bar{E} = \begin{bmatrix} E \\ 0 \end{bmatrix}$$

$$\bar{F}^T = [0 \ a] \quad \bar{D}^T = [0 \ -CB] \quad \bar{C} = [C \ 0 \ 0] \quad \bar{H}^T = [0 \ 0 \ a] \quad \bar{K} = [K_p \ K_d] \quad \bar{C}_e = [-C \ 1]$$

and the variables:

$$\bar{x}^T = [x \ y_{ref_c}] \quad \bar{e}^T = [e \ \dot{e}]$$

From these definitions, come the augmented state equations:

$$\begin{aligned} \dot{\bar{x}} &= \bar{A}\bar{x} + \bar{B}u + \bar{F}y_{ref} + \bar{E}w \\ \bar{e} &= \bar{G}\bar{x} + \bar{D}u + \bar{H}y_{ref} \\ \bar{y} &= \bar{C}\bar{x} \end{aligned}$$

In this new state space, the PD compensator design can be posed as a static output feedback controller design  $u = K\bar{e}$ , where, in closed-loop form:

$$u = (I - K\bar{D})^{-1} K\bar{G}\bar{x} + (I - K\bar{D})^{-1} K\bar{H}y_{ref},$$

which leads to:

$$\begin{aligned} \dot{\bar{x}} &= [\bar{A} + \bar{B}(I - K\bar{D})^{-1} K\bar{G}] \bar{x} + [\bar{F} + \bar{B}(I - K\bar{D})^{-1} K\bar{H}] y_{ref} + \bar{E}w \\ y &= \bar{C}\bar{x} \quad y_{ref} = \bar{C}_e \bar{x} \end{aligned}$$

For convenience, the following matrices are also defined:

$$\tilde{A} = [\bar{A} + \bar{B}(I - K\bar{D})^{-1} K\bar{G}], \quad \tilde{B} = [\bar{F} + \bar{B}(I - K\bar{D})^{-1} K\bar{H}], \quad \tilde{K} = (I - K\bar{D})^{-1} K\bar{G}, \quad \tilde{H} = (I - K\bar{D})^{-1} K\bar{H}$$

## 4.1 Obtaining the Optimized Gains

The objectives of the heading control system are the tracking of a reference input, the attenuation of the disturbance and the reduction of the amount of rolling oscillation during yaw maneuvering and turbulence caused by the slightly damped poles of the lateral dynamics.

Initially we consider a control system whose only control input is the rudder deflection from the tail surfaces. Individual cost objectives, composed of  $\mathcal{H}_2$  and  $\mathcal{H}_\infty$  norms of the transfer functions from the rudder and disturbance to the yaw angle are defined for each linearized model. The multiple models are simultaneously treated in a min-max sense: the overall problem is to minimize the maximum value among the individual objectives. Such framework is motivated by the  $\mathcal{H}_2/\mathcal{H}_\infty$  guaranteed cost PID design technique proposed in [7]. Upper and lower bounds over the proportional-derivative gains of the controller are imposed. Control effort and tracking error are compromised through a single scalar parameter. A constraint over the maximum time constant of the closed loop system is also included.

We defined four performance criteria.

- $J_1 = \|H_{wue}\|_2^2$ :  $\mathcal{H}_2$  norm of the closed-loop transfer function from gust to heading error.
- $J_2 = \|H_{wue}\|_\infty$ :  $\mathcal{H}_\infty$  norm of the closed-loop transfer function from gust to heading error.
- $J_3 = \|H_{rue}\|_2^2$ :  $\mathcal{H}_2$  norm of the closed-loop transfer function from rudder to heading error.
- $J_4 = \|H_{rue}\|_\infty$ :  $\mathcal{H}_\infty$  norm of the closed-loop transfer function from rudder to heading error.

The first two criteria are related to the reduction of the effect of the disturbance and the two next criteria are related with the reduction of the effect of the variation of the reference error. The motivation of mixing  $\mathcal{H}_2$  and  $\mathcal{H}_\infty$  is to use the energy of the signal and the worst-case strategy in a same problem.

The optimization problem is then stated as

$$\begin{aligned} \min_K \max_P J_h(K, P) \quad h = \{1, 2, 3, 4\} \\ s.t \quad \begin{cases} K \in \{\mathcal{K}_\sigma \cap \mathcal{M}\} \\ P \in P_i \quad i = \{1, 2, 3\} \end{cases} \end{aligned} \quad (5)$$

where  $P_i \quad i = \{1, 2, 3\}$  is a set of three linearized models for airship airspeeds of 6, 8 and 10 m/s,

$$\mathcal{K}_\sigma = \left\{ K : \max_{P_i \quad i=\{1,2,3\}} \left( \text{Re} \left[ \lambda \left( \check{A}(K) \right) \right] \right) \leq -\sigma ; \sigma > 0 \right\} \quad (6)$$

is a constraint related with the maximal time constant, and

$$\mathcal{K}_M = \{K : |K_p| \leq K_{pmax}; |K_d| \leq K_{dmax}\} \quad (7)$$

is a constraint related to the maximum admissible absolute values for parameters  $K_p$  and  $K_d$ .

A detailed discussion on how to derive this optimization problem can be found in [7]. With this methodology, the obtained gains are  $K_p = 1.45$  and  $K_d = 3.77$

## 4.2 Simulated Results

The above gains were validated in the airship simulation and control design environment. The mission path was defined as a square with vertices distant 150 m from each other. Wind speed was 1.5 m/s, blowing in the west direction. This data reproduces a flight experiment, which is detailed in Section 5.2<sup>2</sup>.

Figure 5-left shows the trajectory followed by the airship utilizing a proportional gain  $K_p = 3$  and  $K_d = 0$  for the heading controller, while Figure 5-right shows the trajectory followed for the optimized PD gains. As the tracking error is not represented in any performance criterion, there is no improvement on the tracking behavior. On the other hand, in Figure 6 one can see a good improvement in rolling due the changing of the airship heading reference angle. In Figure 7 is presented a simulation result where, even for a smaller ground speed and in the presence of gust, there is reduction of rolling. Figure 8 shows both  $\Psi_{ref}$  and  $\Psi$ , where despite a certain delay the tracking behavior shows a reasonable performance.

<sup>2</sup> In the experiment the wind blows in the southwest direction, but the relative direction with respect to the mission path is the same in both cases.

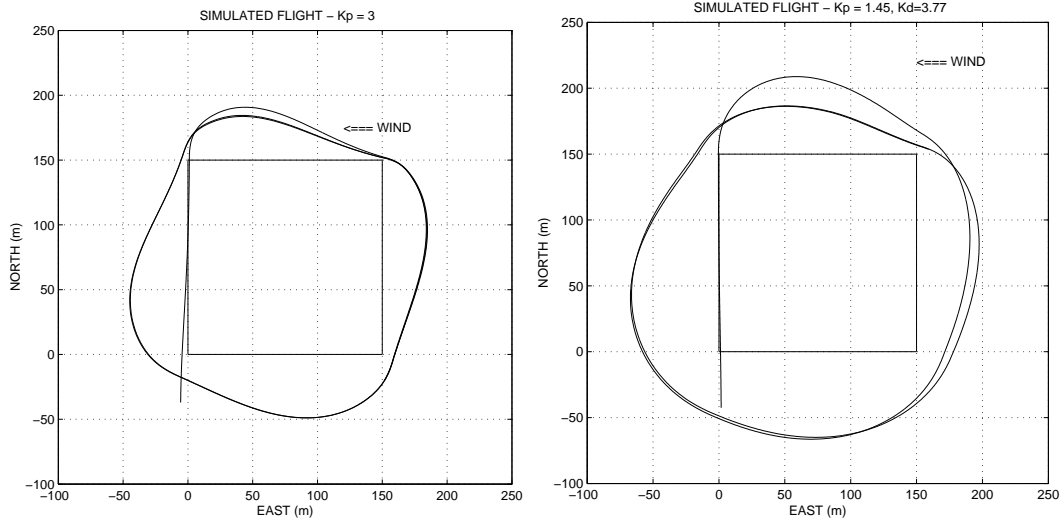


Fig. 5. Trajectory using non-optimized proportional gain (left) and using optimized PD gains (right).

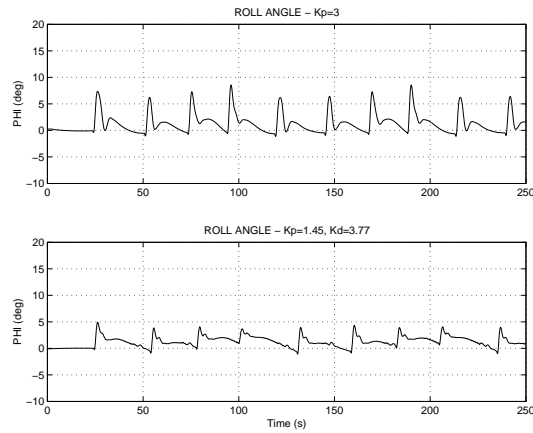


Fig. 6. Rolling angle, 8 m/s ground speed, 1.5 m/s wind speed, no turbulence: non-optimized gain (upper); optimized gains (lower)

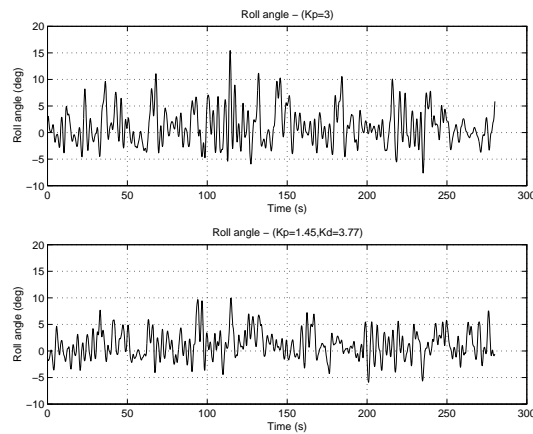


Fig. 7. Rolling angle, 8 m/s ground speed, 1.5 m/s wind speed, with turbulence: non-optimized gain (upper); optimized gains (lower)

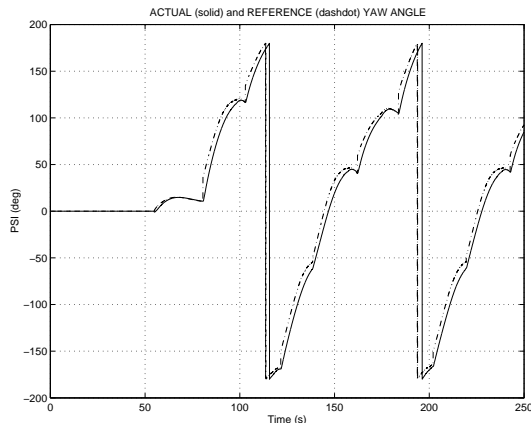


Fig. 8. Reference and actual  $\Psi$  angle.

## 5 Experimental Results

For experimental validation purposes, the PI guidance control method described in Section 3 was implemented in C in the on-board computer. The airship was flown in a military field in Campinas, Brazil. In the sequel one has a brief description of the AURORA I platform, followed by the presentation of the experimental results.

### 5.1 Experimental Platform

AURORA I experimental platform is composed by the AS800 airship shown in Figure 1, and an on-board system, a ground station, and a communication system. Refers to [20] for a detailed description.

*Hardware Infrastructure:* The on-board infrastructure is composed by CPU, inertial sensors and GPS, actuators, and part of the communication system. Most of the components are mounted inside the airship's gondola. The CPU is based on a Pentium 133Mhz PC/104 form factor board, a 10base-T Ethernet network interface, an Emerald MM multi-serial board with four additional serial ports (yielding a total of six serial ports). Except for the on-board GPS receiver, which connects directly to the PC104 bus, all other sensors are connected to the CPU via serial ports and a micro-controller.

*Software Infrastructure* The operational system used is a reduced kernel real time Linux (included in a onboard flash-disk). The software infrastructure is divided into onboard and ground systems. The on-board system is responsible for reading and sending sensor data to the ground station, and for executing automatic control strategies sending commands to the actuators. The ground station is responsible for sending commands, including mission paths, to the on-board station and for receiving sensor data and displaying them in real time during simulated and actual flights. Additionally, the ground system records all data received from the on-board station for post-flight analysis and visualization.

*Communication Infrastructure* The communication system is composed by two radio links. The first one operates in analog mode to transmit video imagery from the airship to the ground station. The second one operates in digital mode to transmit sensor and command data between the ground and on-board stations.

### 5.2 Results

In this experiment, the airship was manually flown for a few minutes before automatic control was switched on. The mission path was defined as a square with vertices distant 150 m from each other. Wind speed was on the range of 0 to 10 km/h, blowing approximately in the southwest direction. The airship velocities and heading, necessary in the control algorithm, were obtained respectively from differential GPS data and compass. Airship path following was controlled automatically by the on-board system, while altitude was

smoothly and manually controlled by the ground pilot. The look-ahead distance used for the controller design was chosen with a reference speed of  $10\text{ m/s}$  and prediction horizon of  $2.5\text{ s}$ :

$$\delta_a = \delta + 25\epsilon \quad (8)$$

The controller’s proportional and integral gains were obtained by trial and error. Figure 9 presents the obtained results. The dotted line represents the airship motion under manual control from take-off until automatic control was switched on. The continuous line represents the airship motion under PI path tracking control. Finally, the dashed line shows the motion of the airship under manual control until landing. In this figure, one can clearly see the adherence to the mission path, as well as an overshoot when the airship turns from southwest to northwest due to the wind disturbance.

Figure 9-right presents one of the airship loops around the square, where the dots represent the airship position and the lines represent its heading. Note that the control method composed by the tracking and heading controllers automatically adjusts the airship heading to compensate for wind disturbances; for example, in the lower left part of the square loop, the airship navigates “sideways”, while in the upper left it navigates mostly facing towards the trajectory. behavior

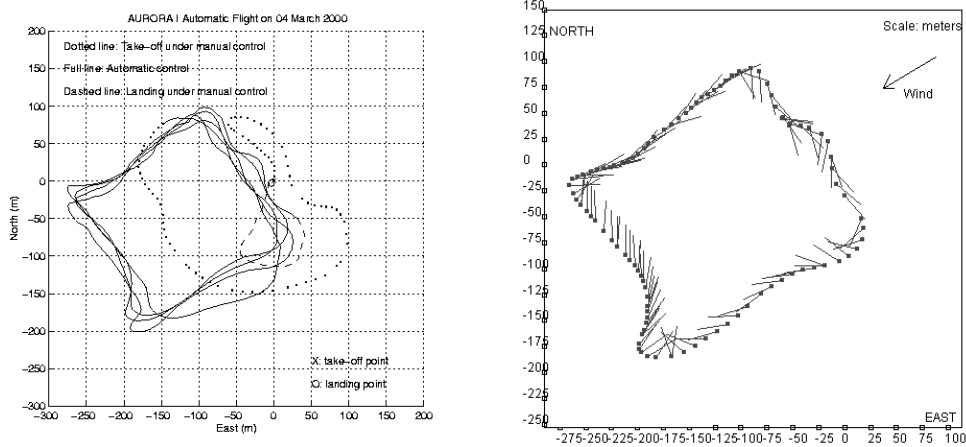


Fig. 9. AURORA I under non-optimized PI control following a set of four points arranged in a square.

## 6 Conclusion

This paper presents a  $\mathcal{H}_2/\mathcal{H}_\infty$  guaranteed cost PD design for the heading controller of the the AURORA I airship. The problem formulation is done considering the same conditions of the first experimental flight, where the objective is to make the vehicle follow a set of pre-defined way points, while reducing the rolling of the airship.

The rolling of the airship during experimental flight has showed to be very large. Then, a optimization approach was used in order to reduce rolling due the airship maneuvering and gust. Simulated results have proved that a considerable improvement is archived in rolling due airship maneuvering. Note that, the reduction of the rolling was a consequence of designing a controller that decreases the influence of the exogenous input in the output (heading angle). This has the advantage of keeping control system the same regarding the non-optimized one, with the drawback of degenerate the tracking of the optimized controller with respect to the non-optimized.

Future works include practical sythesis and validation of the proposed optimized gains in real flight conditions, as well as the design of a decoupled PID airelon controller to archive a great reduction of rolling due gust including the roll angle in the design. Authors intends to flight the actual airship with the optimized gains in the next months.

## Acknowledgments

This work is partially funded by the Brazilian funding agencies FAPESP, under grant nos. 97/13384-7, 98/13563-1, 98/13562-5, 99/04631-6, 99/04645-7, and 00/01000-4, and CNPq under grant no. 68.0140/98-0. It was also supported by the Portuguese Operational Science Program (POCTI), co-financed by European FEDER Program.

## References

1. Netherclift, O.J., *Airships today and tomorrow*, Airship Association Publication no. 4, The Airship Association Ltd., 1993.
2. Elfes, A., Bueno, S.S., Bergerman, M., Ramos, J.J.G., "A Semi-Autonomous Robotic Airship for Environmental Monitoring Missions", *Proceedings of the 1998 IEEE International Conference on Robotics and Automation*, Leuven, Belgium, 1998.
3. Gomes, S.B.V. and Ramos, J.J.G., "Airship Dynamic Modeling for Autonomous Operation", *Proc. of the 1998 IEEE International Conference on Robotics and Automation*, Leuven, Belgium, 1998.
4. De Paiva, Bueno, S.S., Bergerman, M. "A Robust Pitch Attitude Controller for AURORA's Semi-Autonomous Robotic Airship", *13th AIAA Lighter-Than-Air Technology Conference*, Norfolk, VA, USA, 1999.
5. Azinheira, J.R., de Paiva, E.C., Ramos, J.J.G., Bueno, S.S.B. "Mission Path Following for an Autonomous Unmanned Airship", *IEEE Int. Conference on Robotics and Automation - ICRA 2000*, San Francisco, USA, 2000.
6. De Paiva, E.C., Bueno, S.S., Gomes, S.B.V., Ramos, J.J.G. and Bergerman, M. "A Control System Development Environment for AURORA's Semi-Autonomous Robotic Airship", *IEEE Int. Conference on Robotics and Automation - ICRA 1999*, Detroit, MI, USA, May 1999.
7. Takahashi, T.H.C., Peres, P.L.D. and Ferreira, P.A.V. "Multiobjective H<sub>2</sub>/H-infinity Guaranteed Cost PID Design", *IEEE Control Systems Magazine*, October, 1997.
8. McLean, D., *Automatic Flight Control Systems*, Prentice-Hall, 1990.
9. Gomes, S.B.V., "An Investigation of the Flight Dynamics of Airships with Application to the YEZ-2A", *Ph.D. Thesis*, College of Aeronautics, Cranfield University, October 1990.
10. Tan, S.B. and Nagabhushan, B.L. "Robust Heading-Hold Autopilot for an Advanced Airship", *12th AIAA Lighter-Than-Air Technology Conference*, 1997, AIAA-97-1488.
11. Aguilar, L. "Variable structure Control for path following of mobile robots by linearizing techniques." *IFAC Int. Conf. IAV'98*, Madrid, 1998.
12. Azinheira, J. R., Oliveira, H. V., Rocha, B. F. "Aerodynamic measurement system for Project AURORA airship: Calibration Report and User Manual." Mechanical Engineering Institute, Superior Technical Institute, Lisbon, Portugal, 1999. (In Portuguese.)
13. Botto, A., J.R. Azinheira and J. Sá da Costa. "A comparison between robust and predictive autonomous guidance controllers." *Eighteenth IASTED Int. Conf., Innsbruck, Austria*, 1999.
14. de Paiva, E.C., Bueno, S.S., Bergerman, M. "A Robust Pitch Attitude Controller for Aurora's Semi-Autonomous Robotic Airship." *13th AIAA Lighter-Than-Air Systems Tech. Conf.*, Norfolk, VA, 1999.
15. Lourtie, P., J. Azinheira, J.P. Rente and P. Felício. "ARMOR Project - Autonomous Flight Capability." *AGARD FVP95 Specialist Meeting, Design and Operation of Unmanned Air Vehicles*, Turkey, 1995.
16. Mowforth, E. "An introduction to the airship". *Airship Association Publication no. 3*, The Airship Association Ltd., 1991.
17. Munson, K. "Jane's unmanned aerial vehicles and targets". *Jane's Information Group Limited*, Surrey, 1996.
18. NASA National Air and Space Administration. Theseus Project. [www.hq.nasa.gov/office/mtpe/Theseus.html](http://www.hq.nasa.gov/office/mtpe/Theseus.html), 1997.
19. Normey-Rico, J. Gomez Ortega, E.F. Camacho. "Smith-Predictor Based Generalized Predictive Controller for Mobile Robot Path-Tracking", *IFAC Int. Conf. IAV'98*, Madrid, 1998.
20. Ramos, J.J.G. et al. "Project AURORA: a status report." *3rd International Airship Convention and Exhibition*, Friedrichshafen, Germany, July 2000.
21. Ramos, J.J.G., Maeta, S.S., Bergerman, M., Bueno, S.S., Bruciapaglia, A., Mirisola, L.G.B. "Development of a VRML/JAVA unmaned airship simulating environment." *International Conference on Intelligent Robots and Systems*, Kyongju, Korea, Oct. 1999, pp. 1354-1359.
22. Ramos, J.J.G., Bueno, S.S., Maeta, S.M., Paiva, E.C., Asanuma, K., Nascimento, L.G., Bergerman, M., Elfes, A., Beiral, J.A.R. "Project AURORA: autonomous unmanned remote monitoring robotic airship." *2nd International Airship Convention and Exhibition*, Bedford, UK, June 1998, pp. 91-103.

This article was processed using  
the T<sub>E</sub>X macro package with SIRS2001 style